Structural identifiability and practical applicability of an alveolar recruitment model for ARDS patients

C. Schranz[1], P. D. Docherty[2], Y. S. Chiew[2], J. G. Chase[2], K. Möller[1]

[1] Institute for Technical Medicine, Furtwangen University, Villingen-Schwenningen, Germany

[2] Centre for Bioengineering, University of Canterbury, Christchurch, New Zealand

Abstract

Mathematical models of respiratory mechanics can offer substantial insight into patient state and pulmonary dynamics that are not directly measurable. Thus, they offer significant potential to evaluate and guide patient-specific lung protective ventilator strategies for Acute Respiratory Distress Syndrome (ARDS) patients. To assure bedside-applicability, the model has to be computationally efficient and identifiable from the available data, while also capturing dominant dynamics observed in ARDS patients.

In this work, a recruitment model is enhanced by considering alveolar distension and implemented in a time-continuous respiratory mechanics model. A hierarchical gradient decent approach is used to fit the model to low-flow test responses of 12 ARDS patients.

The reported parameter values were physiologically plausible and capable of reproducing the measured pressure responses with high accuracy. Structural identifiability of the model is proven, but a practical identifiability analysis of the results shows a lack of convexity on the error-surface. Covariance analyses reveal limited influence of particular model parameters during parameter identification indicating that successful parameter identification is currently not assured in all test sets.

Overall, the presented model is physiologically and clinically relevant, captures ARDS dynamics, and uses clinically descriptive parameters. The patient-specific models show its ability to capture pulmonary dynamics directly relevant to patient condition and clinical guidance. These characteristics can currently not be directly measured or established without such a validated model.

1. Introduction

In Acute Respiratory Distress Syndrome (ARDS), large regions in the lung can be collapsed [1]. Life support requires mechanical ventilation with high pressures to open and stabilize collapsed alveoli. However, high ventilation pressures may create additional lung damage by overstretching initially opened regions and healthy alveoli [2]. Hence, optimal ventilator settings for individual ARDS patients are an unresolved issue. Furthermore, any settings should be re-evaluated regularly to account for changes in patient condition and physiology [3-4].

To find optimal, patient-specific ventilator settings, mathematical models of respiratory mechanics can be used to predict the outcome of certain ventilator configurations and guide therapy [5-6]. The quality of model predictions depends on the model accuracy itself and the correspondence of the model parameters to the patient properties [7]. To obtain optimal predictions in real-time at the bedside, the model must be computationally efficient and the parameters identifiable from the available information. However, the available patient data is restricted to measurements of airway pressure and flow. Hence, the model must be as simple as possible to remain identifiable, while capturing all necessary dynamics. For ARDS, the dominant dynamics that must be considered include: 1) alveolar recruitment; 2) lung compliance; and 3) alveolar distension at higher pressure causing an effective stiffening of the lung.

Hickling's model of the ARDS lung [8] is an established approach, applied in various forms to describe pressure-volume curves. Markhorst *et al.* [9] performed simulations to predict optimal lung protective airway pressures. Sundaresan *et al.* [10] used a modified version to estimate opening

pressures based on patient data to calculate optimal levels of Positive End-Expiratory Pressure (PEEP).

This paper implements Hickling's recruitment principle in a time-continuous model for the first time enabling simulation of pressure responses with time. Time-continuous simulation of respiratory mechanics offers the ability to link the model to other time-continuous models that are relevant to simulating a patient during mechanical ventilation, such as gas-exchange [11] or cardiovascular models [12-13].

2. Materials & Methods

2.1. Data

Measurements of twelve mechanically ventilated (MV) patients were selected from a previous ARDS – Study, where Low-Flow (LF) manoeuvres were performed using an Evita4Lab-System [14]. During the LF-Manoeuvre the lung is inflated by an extremely low constant gas flow of 33 mL/s until the airway opening pressure reaches 45 mbar, enabling a quasi-static pressure/volume relationship. These measurements consisted of flow rate and airway pressure signals sampled at 125 Hz. The study was approved by the local ethics committees of the participating university hospitals. Informed consent was signed by patients or their legally authorized representative. Please refer to [14] for a detailed description of the experimental setup.

2.2. Model Derivation

The pressure-dependent recruitment model (PRM) developed implements the alveolar recruitment principle according to Hickling [8], and alveolar distension effects as described by Salazar and Knowles [15]. Considering these effects, leads to a nonlinear compliance model that is incorporated into a 1st order model of respiratory mechanics.

2.2.1. 1st Order Model of Respiratory Mechanics (FOM)

The FOM consists of a serial arrangement of a resistance R_{FOM} (mbar·s/mL), representing the airway resistances and resistive tissue contributions, and a compliance C_{FOM} (mL/mbar), which is a measure for the elasticity of the respiratory system (lung and chest wall) [16]. The FOM and the PRM are applied according to volume-controlled ventilation, with the flow rate ($\dot{V} = dV/dt$) in mL/s as the model input, and the airway pressure p_{aw} (mbar) as the model output. The intermediate variable p_a (mbar) represents the alveolar pressure.

$$\dot{p}_a = {C_{FOM}}^{-1} \cdot \dot{V} \quad \text{Eq 1}$$

$$p_{aw} = R_{FOM}\dot{V} + p_a \quad \text{Eq 2}$$

2.2.2. Alveolar Distension Model

Salazar and Knowles described the pressure-volume relationship of lung tissue using an exponential function [15]:

$$V = V_{max}(1 - e^{-p_a K}) \quad \text{Eq 3}$$

where V_{max} (mL) denotes the maximal pulmonary volume and K (1/mbar) describes how fast compliance decreases with increasing pressure. The derivative of Eq 3 with respect to pressure yields the distension model in terms of compliance, thus defining the lung stiffening tissue with pressure increase as an exponential function.

$$C = \frac{dV}{dp_a} = V_{max} K e^{-p_a K} = C_0 e^{-p_a K} \quad \text{Eq 4}$$

2.2.3. Alveolar Recruitment Model

Hickling's recruitment model [8] is based on a lung, divided into N = 30 horizontal layers to capture different levels of superimposed pressure (SP) from SP_n = 0.0 to 14.5 mbar with 0.5 mbar increments. Each layer represents a set of alveolar units that are either recruited ($H_n = 1$) or not recruited ($H_n = 0$), where n corresponds to the layer number (n = 1...30).

$$H_n = \begin{cases} 0, & p_a \leq SP_n + TOP \\ 1, & p_a > SP_n + TOP \end{cases}$$

$$n = 1, 2, 3, \ldots 30 \quad \text{Eq 5}$$

$$SP_n = 0.0, 0.5, 1.0, \ldots 14.5$$

Recruitment is controlled by the Threshold Opening Pressure (*TOP*) which has to be exceeded to recruit alveolar units within a layer in Eq. 5 [10].

As the units of a layer are recruited, their compliance adds up to the overall compliance. The initial compliance of a layer of recruited alveolar units is defined as C_L. At the beginning of an inspiration cycle, a certain amount of alveolar units are initially open, defining the functional residual volume at end-expiration. The overall initial compliance of these alveoli is denoted as C_{FRC}.

2.2.4. Pressure dependent recruitment model (PRM)

The PRM combines alveolar recruitment and distension effects by assigning the compliances C_{FRC} and C_L the compliance-distension function from Salazar-Knowles [15]. This approach yields a pressure-dependent compliance $C_{PRM}(p_a)$ function embedded into the structure of the FOM:

$$\dot{p}_a = C_{PRM}(p_a)^{-1} \cdot \dot{V} = \left[C_{FRC} e^{-Kp_a} + C_L \sum_{n=1}^{30} H_n e^{-K(p_a - SP_n - TOP)} \right]^{-1} \cdot \dot{V} \qquad \text{Eq 6}$$

where p_{aw} in Eq 2 can now be redefined using Eq 6.

2.3. Parameter Identification

The patient-specific parameters of the PRM for identification are defined:

$$X := \{R_{PRM}, C_{PRM}, \Theta, TOP, K\} \qquad \text{Eq 7}$$

where C_{PRM} captures the overall maximal compliance of the completely recruited lung, without considering distension effects defined:

$$C_{PRM} = C_{FRC} + 30C_L \qquad \text{Eq 8}$$

Θ in Eq 7 is a measure of the amount of opened alveolar units before inspiration compared to the overall amount of total units and takes a value from 1.0, for an initially completely recruited lung, to a value of 0.0 for a completely collapsed lung:

$$\Theta = \frac{C_{FRC}}{C_{PRM}} \qquad \text{Eq 9}$$

This notation allows reducing the PRM into a FOM by setting θ and *K* to zero.

Identification of the nonlinear model creates a patient-specific model, and is performed using a gradient-based method that minimizes the sum of squared error (*SSE*) between measured and simulated p_{aw}:

$$SSE = \sum \left(p_{aw,meas} - p_{aw}\right)^2 \qquad \text{Eq 10}$$

With increasing numbers of parameters, a range of parameter constellations or local minima appear as possible solutions. As accurate initial parameter values can significantly reduce the incidence of finding local minima, a hierarchical parameter identification process is applied [17].

The hierarchical method provides more accurate initial values by identifying simpler models with fewer variable parameters first [17]. These first results provide appropriate initial values for the identification of the next, more complex model. Figure 1 shows the overall process schematically.

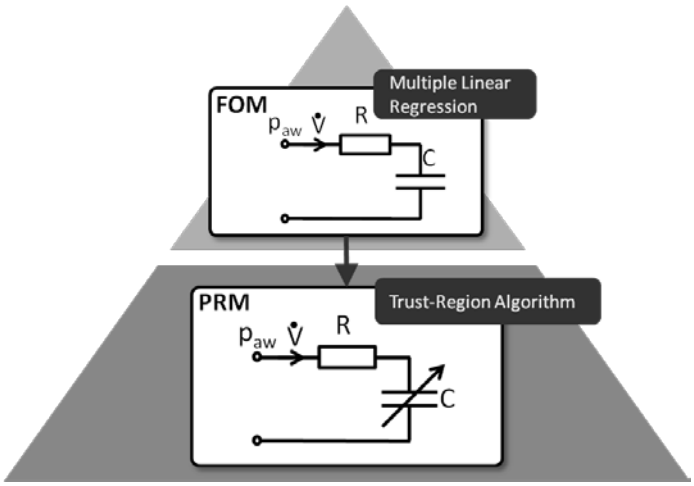

Figure 1: Hierarchical parameter identification of the pressure dependent recruitment model (PRM): Identifying 1st order model of respiratory mechanics (FOM) by multiple linear regression. Use the results to set initial values for the identification of the PRM performed by a gradient-based method (Trust-Region Algorithm).

Combining Eq 2 and the integral of Eq 1 yields R_{FOM} and C_{FOM} in terms of measured variables:

$$p_{aw} = R_{FOM}\dot{V} + {C_{FOM}}^{-1}V \qquad \text{Eq 11}$$

For PRM-Identification, the FOM parameters (R_{FOM}, C_{FOM}) are thus identified using multiple linear regression (MLR):

$$\begin{bmatrix} p_{aw}(1) \\ p_{aw}(2) \\ \vdots \\ p_{aw}(N) \end{bmatrix} = \begin{bmatrix} \dot{V}(1) & V(1) \\ \dot{V}(2) & V(2) \\ \vdots & \vdots \\ \dot{V}(N) & V(N) \end{bmatrix} \begin{bmatrix} R_{FOM} \\ 1/C_{FOM} \end{bmatrix} \qquad \text{Eq 12}$$

Once R_{FOM} and C_{FOM} are identified, they lead to initial values for the PRM identification using a bounded Trust-Region Algorithm (*lsqnonlin* using MATLAB R2011b) [18]. The parameter specific boundaries were set in terms of Eq 7 with X_{LB} = {0, 0, 0, 0, 0} as non-negative lower boundaries and X_{UB} = {1, 1000, 1, 1, 100} as extreme upper boundaries. The initial value of R_{PRM} was set according to R_{FOM}. Θ was set to 0.5 according to general findings in CT-Images of ARDS patients [19-20]. The initial value of K was set arbitrarily to 0.03 1/mbar.

The compliance of the FOM is constant over the measured pressure range, whereas the compliances of the layers in the PRM are exponentially decreasing, with increasing pressure starting from C_{FRC} and C_L, respectively. Assuming that the PRM consists of only a single layer, C_{PRM}, with an initial compliance, $C_{PRM,0}$ the corresponding constant, C_{FOM}, is smaller than $C_{PRM,0}$ and would equal the mean value of the exponentially decreasing compliance C_{PRM} over pressure yielding.

$$C_{PRM} = C_{PRM,0}e^{-Kp_a} \quad \text{Eq 13}$$

$$C_{FOM} = \frac{1}{p_{a,max}}\int_0^{p_{a,max}} C_{PRM,0}e^{-Kp_a}dp_a = \frac{C_{PRM,0}}{p_{a,max}}\left[-\frac{1}{K}e^{-Kp_a,max} + \frac{1}{K}\right] \quad \text{Eq 14}$$

Evaluating the closed integral (Eq 14) and rearranging the equation lead to $C_{PRM,0}$ the initial compliance of the distension model, that is equivalent to the initial value of a pressure decreasing compliance to the constant compliance of the FOM (C_{FOM}):

$$C_{PRM,0} = \frac{KC_{FOM}p_{a,max}}{1 - e^{-Kp_{a,max}}} \quad \text{Eq 15}$$

Currently no *a-priori* information or convenient initial value is available for the *TOP*. Thus, the PRM is identified with initial values for *TOP* ranging from 0 to 12 mbar in 2 mbar increments. The solution with the lowest *SSE* is selected.

To quantify the fitting results, the coefficient of determination (*CD*) was computed:

$$CD = 1 - \frac{SSE}{\sum(p_{aw} - \bar{p}_{aw,meas})^2} \quad \text{Eq 16}$$

The *CD* is a measure of the model goodness-of-fit. A *CD* value of 1.0 corresponds to a perfect model fit and 0.0 means that the model has no relation to the data [16].

2.4. Identifiability Analysis:

2.4.1. Structural Identifiability

Successful parameter identification requires mathematically distinct model parameters [21] and a model should be checked for *a-priori* structural identifiability [22] before it is proposed. *A-priori* structural identifiability states that under ideal noise-free measurements and error-free model structure, the unknown parameters of the postulated model can be uniquely recovered from the measured input-output signals. Structural non-identifiability arises from a redundant parameterization in the model formulation, and ambiguous parameters may be varied without changing the output signal, keeping *SSE* constant [23].

The underlying model was tested for structural identifiability using DAISY [22]. However, DAISY requires the model description in polynomial or rational functions. As the model description of Eq 6 includes exponential terms and Heaviside-Functions, the model was rewritten in polynomial form, with the exponential function approximated by a Taylor Series expansion:

$$e^{-Kp_a} \cong 1 + (-K \cdot p_a) + \frac{(-K \cdot p_a)^2}{2!} + \cdots \qquad \text{Eq 17}$$

The Heaviside-Function (*H*) was first approached by a differentiable logistic function:

$$H_n \cong \frac{1}{1 + e^{-2(p_a - SP_n - TOP)}} \qquad \text{Eq 18}$$

where the exponential function is approximated by another Taylor Series expansion:

$$H_n \cong \frac{1}{1 + 1 + [-2(p_a - SP_n - TOP)] + \frac{[-2(p_a - SP_n - TOP)]^2}{2!} + \cdots} \quad \text{Eq 19}$$

Since the exponential terms of all layers (Eq 6) are distinct, the model was reduced to the basic FRC-Layer of Eq 6 and 2 recruitable layers (n = 1, 2) for simplification to check its structural identifiability. The Taylor series approximations are limited to 3rd order and inserted into the model definition. Higher order polynomials would give better approximations, but have no impact on the proof of identifiability.

As a first step in checking for structural global identifiability for the parameters $p = [R, C_{FRC}, C_L, K, TOP]$ DAISY defines the following ranking amongst the variables:

$$\dot{V} < p_{aw} < \ddot{V} < \ddot{p}_{aw} < p_a < \dot{p}_a \quad \text{Eq 20}$$

Based on the ranking, DAISY calculates the characteristic set of the model. The characteristic set is a family of the differential polynomials A_n belonging to the differential ring

$$R(p)\left[\dot{V}, p_{aw}, p_a\right] \quad \text{Eq 21}$$

The differential polynomials include the input-output relation polynomial, a polynomial with eliminated influence of state variable that only consists of the input and output signals and their derivatives.

By extracting the coefficients of the input-output relation, the exhaustive summary of the model is created. DAISY checks identifiability by solving the algebraic nonlinear equation for the unknown parameters obtained by equating these coefficients to a set of pseudo-randomly chosen numerical

values $p = [\alpha, \beta, \gamma, \delta, \varepsilon]$. The set of equations is solved by the Buchberger algorithm providing the Groebner basis. The Groebner basis allows distinguishing between global or local identifiability or nonidentifiability, if the system admits one solution, a finite number of solutions or infinitely many solutions for each parameter [22, 24].

However, even if structural identifiability is proven, the model may still be non-identifiable [22]. Furthermore, structural identifiability also does not prevent error-mapping methods from being caught in local minima. Hence, structural model identifiability analyses are necessary to prove mathematical distinct model parameters. However, conclusive model evaluation must be undertaken under physiologically realistic conditions.

2.4.2. Practical Identifiability

A structurally identifiable parameter might still be practically non-identifiable if the amount and quality of experimental data is insufficient. This situation is observed if the *SSE* around the global minimum remains below a certain threshold. In a two-dimensional parameter space, practical non-identifiability can be visualized by relatively flat valleys that are infinitely extended. In these regions, changes in *SSE* are negligible, despite significant variation in model parameter values [23]. Practical identifiability analysis was assessed using error-surface analysis and parameter and error covariance analysis.

Error-Surface Matrix Analysis: An error surface matrix *E* around any reported minima was calculated allowing parameter shifts up to ±10% from the reported minima. The error surface was plotted as a function of two model parameters featuring a 0.4% resolution. The resulting plots were arranged in matrix form to visualize the specific influence of each individual parameter on the *SSE* surface.

Parameter Covariance and Error Dependencies Analysis: In addition, the parameter value and error covariance error were measured. Therefore, the particular model parameter was kept constant at a +10% shift from its reported minimum and the remaining parameters are re-identified.

This analysis can be used to asses a number of model structural attributes:

1.) If error changes due to changes in parameter values are negative, it can be concluded that a lower error minimum was found and the parameter identification solution was thus not the global minimum. In this case, parameter identification will be repeated using the values that lead to a lower *SSE* as new initial values.
2.) If the increase in error equals zero due to changes in parameter values, it then may be concluded that the associated variable has no influence in the experiment and is thus non-identifiable. There are two possibilities in such cases:
    - The inter-parameter variances will be zero indicating that the model parameter has no effect on the model output in the given experiment.
    - A significant parameter co-variance will indicate that the model role of the particular parameter can be fully accounted for by another parameter.
3.) If the change in error due to variance in a particular parameter is relatively low, the model parameter may be practically non-identifiable. In such cases either:
    - The particular parameter has only marginal effect on the model output.
    - The parameters model role is partially compensated by another parameter.
4.) If the error shifts significantly with changes in a parameter, the parameter will have a distinct model role

Differential structural model identifiability analyses could capture the second scenario, but would not be able to detect scenario 3. If model non-identifiability was found, the model parameters must be reformulated such that each parameter has a distinct affect on the input-output relationship of the model. If model practical non-identifiability was found, parameter

identification would still be possible. However, the identified parameter values must be treated with caution.

3. Results

While checking for structural identifiability, DAISY calculated 2 polynomials defining the characteristic set.

$$A_1 = f\left(\ddot{V}, \dot{V}, \dot{p}_{aw}, p_{aw}\right)$$
$$= a_1\ddot{V}\dot{V}^6 + a_2\ddot{V}\dot{V}^5 p_{aw} + a_3\ddot{V}\dot{V}^5 + a_4\ddot{V}\dot{V}^4 {p_{aw}}^2 + a_5\ddot{V}\dot{V}^4 p_{aw}$$
$$+ a_6\ddot{V}\dot{V}^4 + \cdots + a_{n-3}\ddot{V}\dot{V} + a_{n-2}\ddot{p}_{aw}\dot{V}^6 + a_{n-1}\ddot{p}_{aw}\dot{V}^5 p_{aw}$$
$$+ a_n\ddot{p}_{aw}\dot{V}^5 + a_{n+1}\dot{V}^4 {p_{aw}}^2 + a_{n+2}\dot{V}^4 p_{aw}$$
$$+ \cdots a_{69}\dot{V}{p_{aw}}^2 + a_{69}\dot{V}p_{aw} + a_{70}\dot{V} \qquad \text{Eq 22}$$

with $a_i = f(R, C_{FRC}, C_L, K, TOP)$:

$$a_1 = -2C_{FRC}K^2R^7$$
$$a_2 = 12C_{FRC}K^2R^6$$
$$a_3 = 4C_{FRC}KR^6(-2K \cdot TOP - 2K - 1)$$
$$\vdots$$
$$a_{70} = 4(-TOP^4 - 4TOP^3 - 7TOP^2 - 6TOP - 3)$$

$$A_2 = f\left(\dot{V}, p_{aw}, p_a\right) = -\dot{V}R - p_a + p_{aw} \qquad \text{Eq 23}$$

A_1 is the input-output polynomial, consisting of 70 summands and A_2 corresponds to Eq 2 equated to zero. The coefficients in Eq 22, $a_1 \ldots a_{70}$ are nonlinear functions on the unknown model parameters. After normalizing A_1, the exhaustive summary, a set of 69 equations was formed. The range set was calculated at pseudo-randomly chosen values $p = [R = 8, C_{FRC} = 5, C_L = 9, K = 6, TOP = 1]$, yielding the following set of 69 algebraic nonlinear equations:

$$
\begin{gathered}
-C_{FRC}K^2R^7 + 377487360 = 0 \\
C_{FRC}K^2R^6 - 47185920 = 0 \\
C_{FRC}KR^6(-2K \cdot TOP - 2K - 1) + 196608000 = 0 \\
\vdots \\
-TOP^4 - 4TOP^3 - 7TOP^2 - 6TOP + 18 = 0
\end{gathered}
\qquad \text{Eq 24}
$$

Solving the system of nonlinear equation provided the following Groebner basis:

$$
R = 8, \quad C_{FRC} = 5, \quad C_L = 9, \quad K = 6, \quad TOP = 1 \qquad \text{Eq 25}
$$

Showing that the parameters have one unique solution, i.e. that the PRM is structural globally identifiable with measurements of airway pressure and flow rate.

The model parameters for each test participant, as well as the cohort statistics are shown in Table 1. In general, the parameter values for the FOM and PRM are within physiologically plausible ranges. By identifying the PRM, the *SSE* of the FOM is decreased by a mean factor of 8.4 [IQR: 3.5-19.4] and high *CD* values close to 1.0 are achieved. The mean computing time of a PRM identification is 44.5 s [IQR: 35.7-75.3] on a desktop PC (Intel Core 2 Duo, 2.80 GHz). The simulated pressure responses of two patient-specific FOM and PRM identification are shown in Fig. 2. The residuals (filtered by moving average t_{width} = 320 ms) of the cohort predictions produced by the FOM and PRM simulation are shown in Figure 3.

Table 1: Resulting model parameter of FOM and PRM identification with reported *SSE* and *CD* value of each subject and cohort variability.

Subject	FOM				PRM						
	R_{FOM} (mbar·s/mL)	C_{FOM} (mL/mbar)	SSE_{FOM} (mbar^2)	CD_{FOM}	R_{PRM} (mbar·s/mL)	C_{PRM} (mL/mbar)	Θ	K (1/mbar)	TOP (mbar)	SSE_{PRM} (mbar^2)	CD_{PRM}
1	0.111	50.54	2294.01	0.995	0.093	96.18	0.48	0.035	4.87	220.64	0.999
2	0.240	49.69	9059.03	0.972	0.138	132.56	0.29	0.056	10.63	785.08	0.996
3	0.129	24.11	4823.81	0.979	0.036	33.90	0.41	0.012	6.57	180.55	0.999
4	0.118	32.42	1654.54	0.995	0.030	45.80	0.24	0.016	0.83	270.07	0.999
5	0.173	41.26	958.61	0.997	0.131	42.97	0.67	0.000	1.01	579.18	0.998
6	0.102	57.58	1651.61	0.997	0.042	75.25	0.46	0.011	1.92	570.56	0.999
7	0.048	62.78	1134.26	0.998	0.052	117.21	0.62	0.028	10.06	427.64	0.999
8	0.186	45.40	7280.36	0.984	0.074	60.80	0.49	0.006	11.04	580.11	0.998
9	0.166	58.50	6367.89	0.987	0.199	123.82	0.54	0.047	2.75	462.06	0.999
10	0.120	64.87	3668.59	0.990	0.049	107.43	0.42	0.023	6.81	682.60	0.998
11	-0.008*	28.34	3497.20	0.987	0.012	50.41	0.46	0.031	0.00	900.35	0.997
12	0.173	56.86	7154.45	0.986	0.080	73.86	0.52	0.005	10.19	704.81	0.998
minimum	-0.008	24.11	958.61	0.972	0.012	33.90	0.24	0.000	0.00	180.55	0.996
Q1	0.107	36.84	1653.08	0.985	0.039	48.11	0.41	0.009	1.46	348.85	0.998
median	0.124	50.12	3582.90	0.989	0.063	74.56	0.47	0.019	5.72	574.87	0.999
Q2	0.173	58.04	6761.17	0.996	0.112	112.32	0.53	0.033	10.12	693.71	0.999
maximum	0.24	64.87	9059.03	0.998	0.199	132.56	0.67	0.056	11.04	900.35	0.999

* Not physiologically plausible

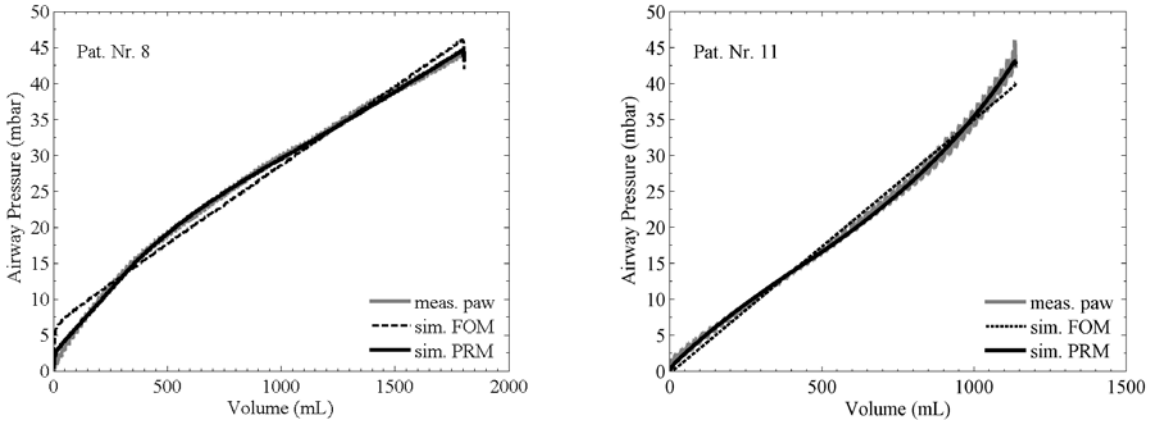

Figure 2: Measured and simulated pressure responses of patient-specific FOM and PRM utilizing the measured flow rate as model input.

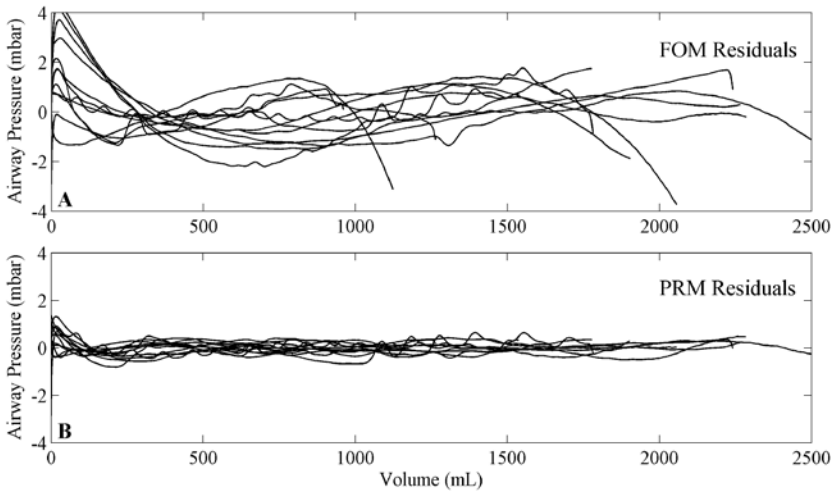

Figure 3: Residuals of FOM and PRM simulations of airway pressure for the overall cohort (N = 12).

The FOM estimates a linear pressure increase around the average of the measured pressure response and leads to acceptable simulation results in patients with linear pressure increase. In subjects where the linear pressure response shows higher deviations from the measured pressure curve, R_{FOM} is overestimated. This result is visible by a pressure step at the beginning of inflation that is too large as seen in Figure 2a.

Figure 3 shows the residuals of FOM simulations of the complete cohort with a median of -0.03 mbar (IQR -0.74 to 0.61; range -3.73 to 4.47). In general, the FOM residuals follow a common wave-shaped pattern being comperatively high initially, lower in the middle of inspiration and higher at end-inspiration. This behaviour indicates unmodeled biased effects. In contrast, PRM simulations produced a median residual of 0.00 mbar (IQR -0.17 to 0.16; range -0.80 to 1.31). The persistent residuals in the PRM case are predominantly caused by cardiogenic oscillations.

The error surface matrix *E* of Subject 1 is shown in Figure 4. The elements in the main diagonal E_{nn} show the rate of change in error by varying a single parameter, where the remaining elements illustrate the change in error by varying two parameters. The error surface is most sensitive to variance in *C* (E_{22}) as it produces the highest rate of change across all variables. In contrast, the error surfaces in the *R* (E_{11}) and *TOP* (E_{55}) dimensions are comparatively flat. These small error dependencies lead to long and flat valleys with limited error gradients in certain directions from the error minima.

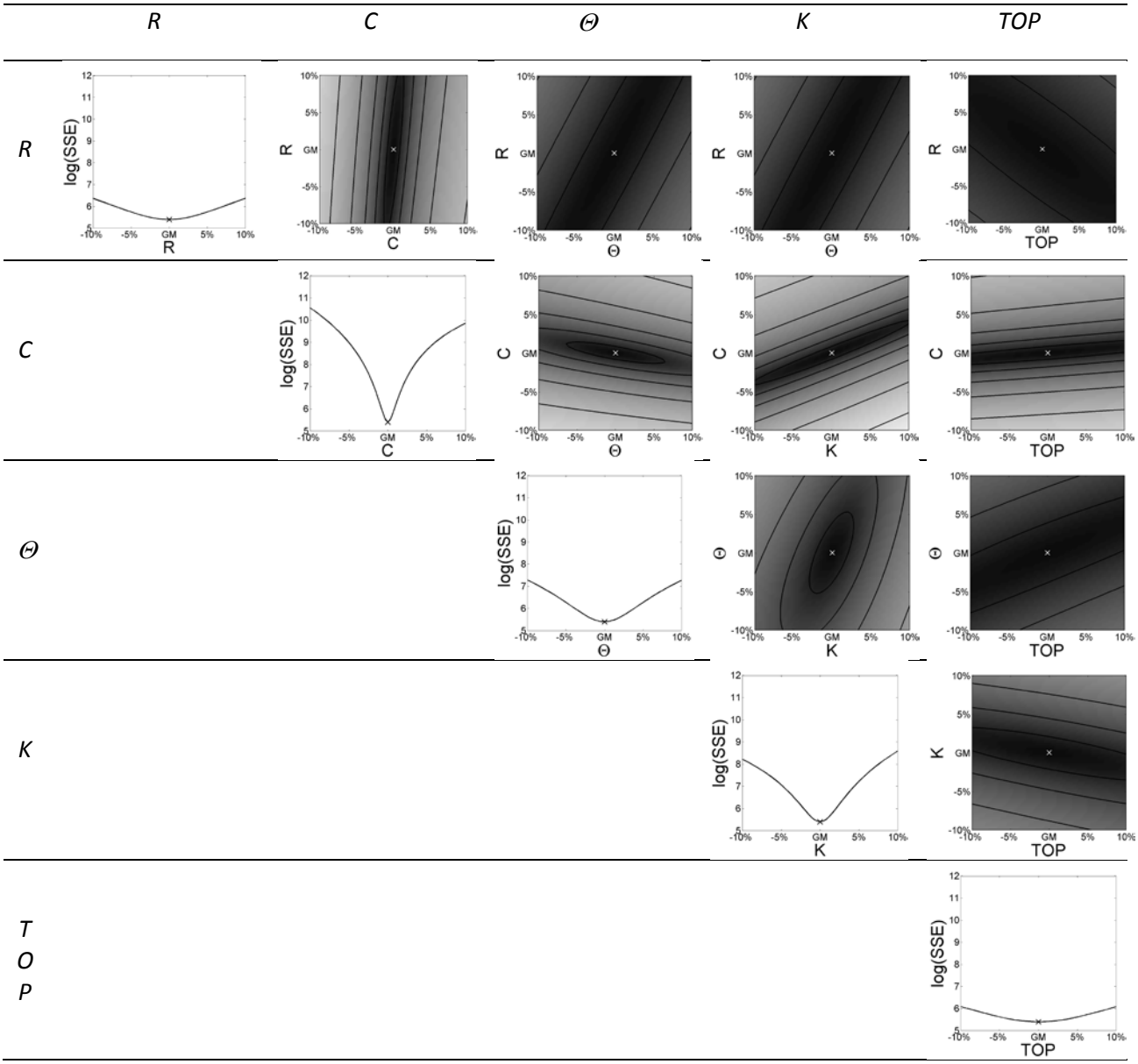

Figure 4: Error surface matrix *E* of subject 1 showing the *SSE* in the vicinity of the global minimum: Each reported parameter value was shifted up to ±10% against each other. Plots with high contrasts indicate high rates of change in error and plots with low contrasts reveal more flat regions.

Parameter covariance and error dependencies analysis performed after the first run of parameter identification revealed negative error-changes in 10 out of 12 data sets and thus caused a restart of the identification process at the new reported minimum.

Over the complete cohort, error was most sensitive to shifts in parameter *C (dSSE/dC)* and showed the lowest error sensitivity to variance in *R* and *TOP (dSSE/dR*, *dSSE/dTOP*). A 10% shift in parameter *C* led to a 30.2% (IQR 13.0% to 60.4%) increase in *SSE*. 10% shifts in *R* and *TOP* caused 4.4% (IQR 1.0% to 10.9%) and 2.5% (IQR 0.3% to 14.8%) changes in *SSE*, respectively. The median change in *SSE* due to a 10% shift in *K* was 6.9% (IQR 1.5% to 38.5%). Parameter covariance analysis also shows that the 10% shift in *R* is predominantly compensated for with a decrease in *TOP* of 6.3% with all other parameters changing less than 1.3%. The highest covariance between parameters was found in *C* and *K* where a 10% shift in *C* is predominantly compensated via a decrease of *K* by 34.2%. Furthermore, a 10% shift in *TOP* led only to marginal shifts in the other parameter smaller than 1.6%. Co-variance analysis indicates that *R* and *TOP* perform similar model functions. Error-dependency analysis reveals a reduced influence of *TOP* in *SSE*.

4. Discussion

The proposed PRM fits the measured data with high accuracy indicated by low residuals and *CD*-values close to 1.0. The model appears able to capture the observed dynamics of ARDS patients with resulting parameter values consistently within physiological ranges. The FOM also provides good model fits as seen in Figure 2. However, the FOM residuals (Figure 3) indicate consistent bias patterns that could be eliminated by the PRM.

The physical principles captured in the PRM representing the dynamics at the alveolar scale. The model features recruitment effects, as well as alveolar distension, and allows continuous simulations of respiratory mechanics with respect to time. Each model parameter is directly, physiologically relevant and highly descriptive. *R* and *C* offer clinically important insights into the overall airway resistance and lung stiffness. Parameter *K* is a measurement of how fast a lung unit reaches over-inflation with respect to increasing pressure. Thus, a relatively high value of *K* would mean that over distension can be reached even in low pressure regions, whereas low values of *K* would indicate that over-inflation is a risk at higher pressures. Θ and *TOP* describe the alveolar recruitability. Θ offers estimates on the fraction of initially recruited alveoli within the lung compared to the total number of alveoli and *TOP* seems to be highly relevant in terms of recruitability to guide clinical decision making [6].

In data sets wherein the experimental protocol did not cause an upwards convexity in the pressure response, the reported values for *K* approach 0.0. Note that the range of *dSSE/dK* was relatively large. This was due to the lack of distension which occurred in some experiments. In such cases, *K* is considered to be practically unidentifiable due to missing information content within these measured data. To ensure that the dataset has sufficient information to reliably identify *K*, the tidal

volume can be increased to cause some evidence of over-inflation and a resulting distinct upwards convexity in the pressure response. However, clinically these kinds of manoeuvres would lead to high ventilation pressures that might be harmful for the subject and are thus unlikely in a clinical setting. Hence, a compromise between risks and benefits for quantifying distension properties at the bedside must be found.

The basic FOM provided relatively accurate estimates in patients with quasi-linear pressure responses as first step of the hierarchical parameter identification. In subjects with highly curved pressure responses, the FOM simulation matches the measurement quantitatively well. The patient-specific pressure responses lay in the average around the measured pressure minimizing the overall deviation. In four out of 12 subjects, the parameter identification of the FOM overestimates the resistance to compensate for nonlinearities in the compliance leading to higher deviations from the observed behaviour in low pressures regions (Figure 2a). In Subject 11, FOM identification reported a negative, non-physiological resistance value (Figure 2b). Equally non-physiological values can be readily avoided using bounded search methods for the FOM identification

In general, the hierarchical parameter identification process sets effective initial values for *R* and *C* in the first step. However, the overall computational cost of parameter identification is relatively high due to the lack of convexity in the *TOP* error plane (Figure 4) and the lowest contribution of *TOP* to model error in the co-variance. Thus, parameter identification was initiated at various equidistant initial values of *TOP* along a physiologically plausible range. It may be possible to locate a suitable starting value for *TOP* in a hierarchical manner similar to *C* and *R* [10]. However, no such simpler model has been proposed at this stage. Likewise Electro-Impedance Tomography (EIT) would also be able to provide estimates on *TOP* directly at the bedside [4].

The error-dependencies analysis revealed that if model error was evaluated with 10% shift in single parameter values, a new solution with a lower *SSE* was found in some cases. This behaviour indicates premature parameter-identification convergence declaration since lower error minima could be detected. This was a failure of the parameter identification methodology. It seems that the relatively flat error-surface impaired the gradient-based parameter identification method. When negative error changes occurred, the parameter identification was rerun from that point until no new solution with a lower *SSE* was found. However, given the lack of convexity observed in the parameter error planes (Figure 4), it is not possible to guarantee that a true global minimum was found.

By analysing the error-surface matrix of Subject 1 in Figure 4, the relatively wide flat regions and long flat valleys are visible. Gradient-based algorithms can occasionally terminate as soon as these flat regions are approached, leading to parameter values relatively far from a true minimum. These wide flat regions are mainly observed in terms of the variables *R* and *TOP*, since these two show the flattest surface. The *C* vs. *R* or *TOP* error planes show long valleys with low gradient. An error-map matrix of Subject 3 (not shown) reveals particularly flat error surfaces around the reported minimum with respect to *R* and *TOP*. A significant *SSE* dependence could only be observed in the parameter *C* for this subject. These outcomes emphasise the difficulties parameter identification of this specific model when the characteristics which the model is designed to capture are not present in the data set.

According to the error-surface matrix, *C* seems to be the most convex parameter with respect to error. This finding in Subject 1 could be confirmed by error-dependency analyses, revealing that a

shift in *C* led to the highest error increase amongst all parameters when identification is redone with the altered *C* value. However, changes in *TOP* show almost no influence in *SSE* or the other parameters, explaining the necessity of a grid search algorithm for parameter identification at various *TOP* starting values. Due to the occasional lack of information in the dataset for parameter *K* and the low convexity regarding parameter *R* and *TOP*, the system can suffer model identifiability and parameter identification problems.

While, the PRM proved to be globally identifiable using DAISY, it can be shown that practical identifiability of the proposed model was not assured with the available airway pressure and flow rate data. Therefore, further investigation is necessary to verify whether the model should be re-formulated to simplify parameter identification. In particular, it may be reasonable to suspect that a resistive influence might be negligible during low-flow experiments. Thus, according to covariance analysis, eliminating *R* from the model may lead to an increased sensitivity in *TOP* and would probably improve overall identifiability.

In the cases wherein the dataset allowed robust identification of the PRM parameters, the model successfully captured the respiratory pressure-volume kinetics by modelling mechanics down in the alveolar scale. Hence in these cases, the physiological insight gained from the model could potentially be used to optimise ventilator therapy. However, in cases where in the dataset did not contain sufficient information for robust model identification, the identified PRM parameters values were of limited value. If the practical identifiability of the model is improved, the PRM will be more universally useful in a clinical environment, as it offers highly accurate model simulations and physiologically meaningful patient-specific parameters. The PRM model requires only measurements of airway pressure and flow rates that are readily available and non-invasive obtained. However, the

physiological interpretations of the model parameters are only valid if the model assumptions are correct. Although, the true recruitment mechanisms are still unknown, several clinical studies [4, 25-26] support the recruitment principle according to Hickling's definition.

Thus, the gained information is clinically and physiologically relevant in the evaluation of lung protective settings and strategies. It can also be used to guide therapeutic decisions and MV settings. For example, using the model of Sundaresan *et al* [6], a large decrease in *TOP* with added PEEP implies that additional PEEP produces additional recruitment of new alveoli units. Thus, the model presented here would add utility to these already validated models in setting PEEP. The model also provides time-continuous simulations of various flow rates. Therefore, it has added potential to be implemented as an additional submodel, interacting with additional physiological models in dynamically generated models for medical decision support for mechanical ventilation [12, 27].

5. Conclusion

A direct, physiologically relevant model was proposed that is able to fit the observed dynamics of ARDS patients with high accuracy. The model parameters are descriptive, clinically relevant and show significant potential to provide unique insight to guide therapy and support lung protective ventilation strategies. Its structural identifiability is proven assuring successful parameter identification under noise-free data and error-free model structure. However, in practical applications with noisy data, the model appears over-parameterised and is not practically identifiable in some cases. The problem is exacerbated where no distension effects could be reached. To increase the models utility more robust parameter identification is required. Hence, a model reformulation should be considered. Overall, this well known recruitment principle, implemented in a time-continuous model is theoretically identifiable and accurately describes observed clinical dynamics of ARDS patients. Optimal ventilation management and continuous patient monitoring may profit from further investigations in applying this model in conjunction with others to evaluate and guide mechanical ventilation therapy.

Acknowledgments

The authors express their gratitude to the McREM Study Group and Dräger Medical for providing the data for this retrospective study. This work was supported by the Deutsche Forschungsgemeinschaft DFG under Grant MO 579/1-2 PAR (Protective Artificial Respiration) and the German Academic Exchange Service (DAAD).

References

[1] D. G. Ashbaugh, D. B. Bigelow, T. L. Petty, and B. E. Levine, "Acute respiratory distress in adults," Lancet, vol. 2, pp. 319-23, Aug 12 1967.

[2] L. Gattinoni, P. Caironi, M. Cressoni, D. Chiumello, V. M. Ranieri, M. Quintel, *et al.*, "Lung recruitment in patients with the acute respiratory distress syndrome," N Engl J Med., vol. 354, pp. 1775-86, 2006.

[3] R. G. Brower, A. Morris, N. MacIntyre, M. A. Matthay, D. Hayden, T. Thompson, *et al.*, "Effects of recruitment maneuvers in patients with acute lung injury and acute respiratory distress syndrome ventilated with high positive end-expiratory pressure," Crit Care Med, vol. 31, pp. 2592-7, Nov 2003.

[4] S. Pulletz, A. Adler, M. Kott, G. Elke, B. Gawelczyk, D. Schadler, *et al.*, "Regional lung opening and closing pressures in patients with acute lung injury," J Crit Care, vol. (in press), Oct 25 2011.

[5] S. Lozano, K. Möller, A. Brendle, D. Gottlieb, S. Schumann, C. A. Stahl, *et al.*, "AUTOPILOT-BT: a system for knowledge and model based mechanical ventilation," Technol Health Care., vol. 16, pp. 1-11, 2008.
[6] A. Sundaresan, J. G. Chase, G. M. Shaw, Y. S. Chiew, and T. Desaive, "Model-based optimal PEEP in mechanically ventilated ARDS patients in the intensive care unit," Biomed Eng Online, vol. 10, p. 64, 2011.
[7] J. G. Chase, A. J. Le Compte, J. C. Preiser, G. M. Shaw, S. Penning, and T. Desaive, "Physiological modeling, tight glycemic control, and the ICU clinician: what are models and how can they affect practice?," Ann Intensive Care, vol. 1, p. 11, 2011.
[8] K. G. Hickling, "The pressure-volume curve is greatly modified by recruitment. A mathematical model of ARDS lungs," Am J Respir Crit Care Med., vol. 158, pp. 194-202, 1998.
[9] D. G. Markhorst, H. R. van Genderingen, and A. J. van Vught, "Static pressure-volume curve characteristics are moderate estimators of optimal airway pressures in a mathematical model of (primary/pulmonary) acute respiratory distress syndrome," Intensive Care Med, vol. 30, pp. 2086-93, Nov 2004.
[10] A. Sundaresan, T. Yuta, C. E. Hann, J. G. Chase, and G. M. Shaw, "A Minimal Model of Lung Mechanics and Model based Markers for Optimizing Ventilator Treatment in ARDS Patients," Comput Methods Programs Biomed., vol. 95, pp. 166-80, 2009.
[11] S. E. Rees, S. Kjaergaard, P. Perthorgaard, J. Malczynski, E. Toft, and S. Andreassen, "The automatic lung parameter estimator (ALPE) system: non-invasive estimation of pulmonary gas exchange parameters in 10-15 minutes," J Clin Monit Comput, vol. 17, pp. 43-52, Jan 2002.
[12] J. Kretschmer, A. Wahl, and K. Moller, "Dynamically generated models for medical decision support systems," Comput Biol Med, vol. 41, pp. 899-907, Oct 2011.
[13] C. Starfinger, J. G. Chase, C. E. Hann, G. M. Shaw, P. Lambert, B. W. Smith, *et al.*, "Prediction of hemodynamic changes towards PEEP titrations at different volemic levels using a minimal cardiovascular model," Comput Methods Programs Biomed, vol. 91, pp. 128-34, Aug 2008.
[14] C. A. Stahl, K. Möller, S. Schumann, R. Kuhlen, M. Sydow, C. Putensen, *et al.*, "Dynamic versus static respiratory mechanics in acute lung injury and acute respiratory distress syndrome," Crit Care Med., vol. 34, pp. 2090-8, 2006.
[15] E. Salazar and J. H. Knowles, "An analysis of pressure-volume characteristics of the lungs," J Appl Physiol., vol. 19, pp. 97-104, 1964.
[16] J. H. Bates, Lung Mechanics: An Inverse Modeling Approach, 1 ed.: Cambridge University Press, 2009.
[17] C. Schranz, C. Knöbel, J. Kretschmer, Z. Zhao, and K. Möller, "Hierarchical Parameter Identification in Models of Respiratory Mechanics," IEEE Trans Biomed Eng., vol. 58, pp. 3234-41, 2011.
[18] T. F. Coleman and Y. Li, "An Interior, Trust Region Approach for Nonlinear Minimization Subject to Bounds," SIAM J Optimiz., vol. 6, pp. 418-445, 1996.
[19] G. Bugedo, A. Bruhn, G. Hernandez, G. Rojas, C. Varela, J. C. Tapia, *et al.*, "Lung computed tomography during a lung recruitment maneuver in patients with acute lung injury," Intensive Care Med, vol. 29, pp. 218-25, Feb 2003.
[20] G. M. Albaiceta, F. Taboada, D. Parra, L. H. Luyando, J. Calvo, R. Menendez, *et al.*, "Tomographic study of the inflection points of the pressure-volume curve in acute lung injury," Am J Respir Crit Care Med, vol. 170, pp. 1066-72, Nov 15 2004.
[21] P. D. Docherty, J. G. Chase, T. F. Lotz, and T. Desaive, "A graphical method for practical and informative identifiability analyses of physiological models: a case study of insulin kinetics and sensitivity," Biomed Eng Online, vol. 10, p. 39, 2011.
[22] G. Bellu, M. P. Saccomani, S. Audoly, and L. D'Angio, "DAISY: A new software tool to test global identifiability of biological and physiological systems," Comput. Methods Prog. Biomed., vol. 88, pp. 52-61, 2007.
[23] A. Raue, C. Kreutz, T. Maiwald, J. Bachmann, M. Schilling, U. Klingmuller, *et al.*, "Structural and practical identifiability analysis of partially observed dynamical models by exploiting the profile likelihood," Bioinformatics, vol. 25, pp. 1923-9, Aug 1 2009.
[24] M. P. Saccomani, S. Audoly, G. Bellu, and L. D'Angiò, "Examples of testing global identifiability of biological and biomedical models with the DAISY software," Comput Biol Med., vol. 40, pp. 402-7, 2010.
[25] S. Crotti, D. Mascheroni, P. Caironi, P. Pelosi, G. Ronzoni, M. Mondino, *et al.*, "Recruitment and derecruitment during acute respiratory failure: a clinical study.," Am J Respir Crit Care Med., vol. 1, pp. 131-40, 2001.
[26] H. J. Schiller, J. Steinberg, J. Halter, U. McCann, M. DaSilva, L. A. Gatto, *et al.*, "Alveolar inflation during generation of a quasi-static pressure/volume curve in the acutely injured lung," Crit Care Med, vol. 31, pp. 1126-33, Apr 2003.
[27] A. Sundaresan and J. G. Chase, "Positive End Expiratory Pressure in patients with Acute Respiratory Distress Syndrome – The past, present and future," Biomed Signal Proces, vol. to appear, 2011.